






Cite this: *Green Chem.*, 2023, **25**, 10436

## A comparative study of palladium-gold and palladium-tin catalysts in the direct synthesis of H<sub>2</sub>O<sub>2</sub>†

Dávid Kovačič,<sup>‡a</sup> Richard J. Lewis,<sup>‡a</sup>  <sup>‡a</sup> Caitlin M. Crombie,<sup>a</sup> David J. Morgan,<sup>‡a,b</sup> Thomas E. Davies,<sup>a</sup> Ángeles López-Martín,<sup>a</sup> Tian Qin,<sup>c</sup> Christopher S. Allen,<sup>f,g</sup> Jennifer. K. Edwards,<sup>‡d</sup> Liwei Chen,<sup>c</sup> Martin Skov Skjøth-Rasmussen,<sup>e</sup> Xi Liu  <sup>\*c</sup> and Graham J. Hutchings  <sup>\*a</sup>

Herein we evaluate the promotive effect of Au and Sn incorporation into supported Pd nanoparticles for the direct synthesis of H<sub>2</sub>O<sub>2</sub> from molecular H<sub>2</sub> and O<sub>2</sub>. The introduction of both secondary metal modifiers was found to result in a significant enhancement in catalytic performance, although, in the case of the PdSn system, it was identified that relatively large quantities of the secondary metal were required to rival the activity observed over optimal Au-containing formulations, with the 0.25%Pd–2.25%Sn/TiO<sub>2</sub> catalyst offering comparable H<sub>2</sub>O<sub>2</sub> synthesis rates to the optimised 0.25%Pd–0.25%Au/TiO<sub>2</sub> formulation. The introduction of Sn was found to considerably improve Pd dispersion, correlating with an improvement in selective H<sub>2</sub> utilisation. Notably, the optimal PdSn catalyst identified in this work achieves superior H<sub>2</sub>O<sub>2</sub> selectivities compared to the PdAu analogue and is able to rival the performance of *state-of-the-art* materials.

Received 2nd October 2023,  
Accepted 13th November 2023  
DOI: 10.1039/d3gc03706a

rsc.li/greenchem

## Introduction

Hydrogen peroxide (H<sub>2</sub>O<sub>2</sub>) is a highly efficacious, environmentally friendly oxidant, used widely in sectors ranging from textile and paper manufacture, where its strong bleaching properties are sought,<sup>1</sup> to chemical synthesis,<sup>2,3</sup> where H<sub>2</sub>O<sub>2</sub> is superseding traditional reagents, such as perchlorate or permanganate. Indeed, the use of H<sub>2</sub>O<sub>2</sub> in chemical valorisation is particularly attractive, given that the only by-product of its use is water, reducing separation costs associated with stoichiometric oxidants and typically allowing for the use of lower reaction temperatures compared to alternative aerobic routes.<sup>4,5</sup>

The current demand for H<sub>2</sub>O<sub>2</sub> is met almost entirely *via* the anthraquinone oxidation (AO) process. Although, highly efficient there are several concerns associated with the industrial route, in particular around its atom efficiency, with the over-hydrogenation of the anthraquinone H<sub>2</sub> carrier necessitating its periodic replacement.<sup>6</sup> This coupled with the overall complexity of the process has typically precluded the production of H<sub>2</sub>O<sub>2</sub> at the point of final application. As such H<sub>2</sub>O<sub>2</sub> is shipped at concentrations far greater than that required by the end user, with the resulting dilution of the oxidant prior to use effectively wasting the energy utilised in its distillation and concentration before transit. Furthermore, the instability of H<sub>2</sub>O<sub>2</sub>, with its rapid decomposition to H<sub>2</sub>O in the presence of relatively mild temperatures or weak bases requires the use of acidic stabilizing agents to prolong shelf-life,<sup>7</sup> with such species often promoting reactor corrosion and catalyst deactivation.<sup>8</sup>

Alternatively, the direct synthesis of H<sub>2</sub>O<sub>2</sub> from its constituent elements would allow for on-site production, at appropriate concentrations, while avoiding the use of additives and the costs associated with the transport and storage of the oxidant.<sup>9,10</sup> Indeed there is a growing interest in the use of

<sup>a</sup>Max Planck–Cardiff Centre on the Fundamentals of Heterogeneous Catalysis FUNCAT, Cardiff Catalysis Institute, School of Chemistry, Cardiff University, Cardiff, CF24 4HQ, UK. E-mail: LewisR27@cardiff.ac.uk, LiuXi@sjtu.edu.cn, Hutch@cardiff.ac.uk

<sup>b</sup>Harwell XPS, Research Complex at Harwell (RCaH) Didcot, OX11 0FA, UK

<sup>c</sup>In-situ Centre for Physical Sciences, School of Chemistry and Chemical, Frontiers Science Centre for Transformative Molecules, Shanghai 200240, P. R. China

<sup>d</sup>Cardiff Catalysis Institute, School of Chemistry, Cardiff University, Main Building, Park Place, Cardiff, CF10 3AT, UK

<sup>e</sup>Haldor Topsøe A/S, Haldor Topsøes Allé 1, DK-2800 Kongens Lyngby, Denmark

<sup>f</sup>Electron Physical Sciences Imaging Centre, Diamond Light Source Ltd, Didcot, OX11 0DE, UK

<sup>g</sup>Department of Materials, University of Oxford, Oxford, OX1 3PH, UK

†Electronic supplementary information (ESI) available. See DOI: <https://doi.org/10.1039/d3gc03706a>

‡These authors contributed equally to this work.



H<sub>2</sub>O<sub>2</sub> generated *in situ* for use in chemical transformations.<sup>11–13</sup> While Pd-based catalysts have been well reported to offer high activity towards H<sub>2</sub>O<sub>2</sub> production *via* the direct route,<sup>14,15</sup> limited catalytic selectivity has typically necessitated the use of acidic or halogenated stabilising agents.<sup>16–19</sup> Alternatively, there has been extensive investigation into the alloying of Pd with secondary metals, primarily other precious metals<sup>20–24</sup> to improve catalytic performance. The alloying of Pd with Au in particular has been shown to greatly enhance catalytic selectivity towards H<sub>2</sub>O<sub>2</sub>, through isolation and electronic effects, while also avoiding the need for the stabilising agents often required by Pd catalysts.<sup>21,25,26</sup>

In recent years numerous studies have reported that enhancements in catalytic performance similar to those achieved through the alloying of Pd with Au can be achieved *via* the incorporation of a range of Earth-abundant metals.<sup>27–31</sup> The use of such secondary metal modifiers for Pd represents a key step towards an industrially viable route to the direct synthesis of H<sub>2</sub>O<sub>2</sub>. In particular, the use of PdSn formulations has received growing attention, with a number of catalyst formulations reported to offer high selectivity and activity towards H<sub>2</sub>O<sub>2</sub>.<sup>27,32–34</sup> With these earlier studies in mind and with the aim of gaining further understanding of this relatively new class of catalytic materials we now investigate the efficacy of a series of bimetallic PdSn and PdAu catalysts for the direct synthesis of H<sub>2</sub>O<sub>2</sub>.

## Experimental

### Catalyst preparation

Mono- and bi-metallic PdX/TiO<sub>2</sub> (X = Au, Sn) catalysts, were prepared on a weight basis, *via* a wet co-impregnation procedure, based on a methodology previously reported in the literature.<sup>35</sup> With catalysts produced *via* such a procedure widely studied for the direct synthesis of H<sub>2</sub>O<sub>2</sub> due to the simplicity and ease with which this approach can be scaled to meet industrial application. The procedure to produce the 0.25% Pd–0.25%Au/TiO<sub>2</sub> (2 g) catalyst is detailed below, with a similar approach utilized for all mono- and bi-metallic catalysts studied, using chloride-based metal precursors in all cases.

Aqueous PdCl<sub>2</sub> solution (0.833 mL, [Pd] = 6 mg mL<sup>-1</sup>, Merck) and aqueous HAuCl<sub>4</sub>·3H<sub>2</sub>O solution (0.408 mL, [Au] = 12.25 mg mL<sup>-1</sup>, Strem Chemicals) were mixed in a 50 mL round-bottom flask and heated to 65 °C with stirring (1000 rpm) in a thermostatically controlled oil bath, with total volume fixed to 16 mL using H<sub>2</sub>O (HPLC grade). Upon reaching 65 °C, TiO<sub>2</sub> (1.98 g, Degussa, P25) was added over the course of 5 minutes, with constant stirring. The resulting slurry was stirred at 65 °C for a further 15 minutes, following this the temperature was raised to 95 °C for 16 h to allow for complete evaporation of water. The resulting solid was ground prior to an oxidative heat treatment (static air, 400 °C, 3 h, 10 °C min<sup>-1</sup>).

In the case of the PdSn/TiO<sub>2</sub> catalyst series SnCl<sub>4</sub>·5H<sub>2</sub>O ([Sn] = 5.0 mgmL<sup>-1</sup>, Merck) was utilised as the Sn precursor.

The surface area of key catalysts studied, as determined by 5-point BET analysis is reported in Table S.1.†

### Catalyst testing

**Note 1:** The reaction conditions used within this study operate under the flammability limits of gaseous mixtures of H<sub>2</sub> and O<sub>2</sub>.<sup>36</sup>

**Note 2:** The conditions used within this work for H<sub>2</sub>O<sub>2</sub> synthesis and degradation have previously been investigated, with the presence of CO<sub>2</sub> as a diluent for reactant gases and a methanol co-solvent identified as key to maintaining high catalytic efficacy towards H<sub>2</sub>O<sub>2</sub> production.<sup>37</sup> In particular the CO<sub>2</sub> gaseous diluent, has been found to act as an *in situ* promoter of H<sub>2</sub>O<sub>2</sub> stability through dissolution in the reaction medium and the formation of carbonic acid. We have previously reported that the use of the CO<sub>2</sub> diluent has a comparable promotive effect to that observed when acidifying the reaction solution to a pH of 4 using HNO<sub>3</sub>.<sup>38</sup>

### Direct synthesis of H<sub>2</sub>O<sub>2</sub>

Hydrogen peroxide synthesis was evaluated using a Parr Instruments stainless steel autoclave with a nominal volume of 50 mL, equipped with a PTFE liner (so that the total volume is reduced to 33 mL), and a maximum working pressure of 2000 psi. To test each catalyst for H<sub>2</sub>O<sub>2</sub> synthesis, the autoclave liner was charged with catalyst (0.01 g) and solvent (methanol (5.6 g, HPLC grade, Fischer Scientific) and H<sub>2</sub>O (2.9 g, HPLC grade, Fischer Scientific)). The charged autoclave was then purged three times with 5% H<sub>2</sub>/CO<sub>2</sub> (100 psi) before filling with 5% H<sub>2</sub>/CO<sub>2</sub> to a pressure of 420 psi, followed by the addition of 25% O<sub>2</sub>/CO<sub>2</sub> (160 psi), with the pressure of 5% H<sub>2</sub>/CO<sub>2</sub> and 25% O<sub>2</sub>/CO<sub>2</sub> given as gauge pressures. The reaction was conducted at a temperature of 20 °C for 0.5 h with stirring (1200 rpm). H<sub>2</sub>O<sub>2</sub> productivity was determined by titrating aliquots of the final solution after reaction with acidified Ce(SO<sub>4</sub>)<sub>2</sub> (0.0085 M) in the presence of ferroin indicator. Catalyst productivities are reported as mol<sub>H<sub>2</sub>O<sub>2</sub></sub> kg<sub>cat</sub><sup>-1</sup> h<sup>-1</sup>.

The catalytic conversion of H<sub>2</sub> and selectivity towards H<sub>2</sub>O<sub>2</sub> were determined using a Varian 3800 GC fitted with TCD and equipped with a Porapak Q column.

H<sub>2</sub> conversion (eqn (1)) and H<sub>2</sub>O<sub>2</sub> selectivity (eqn (2)) are defined as follows:

$$\text{H}_2\text{Conversion}(\%) = \frac{\text{mmol}_{\text{H}_2}(t(0)) - \text{mmol}_{\text{H}_2}(t(1))}{\text{mmol}_{\text{H}_2}(t(0))} \times 100 \quad (1)$$

$$\text{H}_2\text{O}_2\text{ Selectivity}(\%) = \frac{\text{H}_2\text{O}_2\text{ detected}(\text{mmol})}{\text{H}_2\text{ consumed}(\text{mmol})} \times 100. \quad (2)$$

The total autoclave capacity was determined *via* water displacement to allow for accurate determination of H<sub>2</sub> conversion and H<sub>2</sub>O<sub>2</sub> selectivity.



### Gas replacement experiments for the direct synthesis of H<sub>2</sub>O<sub>2</sub>

An identical procedure to that outlined above for the direct synthesis reaction was followed for a reaction time of 0.5 h. After this, stirring was stopped and the reactant gas mixture was vented prior to replacement with the standard pressures of 5% H<sub>2</sub>/CO<sub>2</sub> (420 psi) and 25% O<sub>2</sub>/CO<sub>2</sub> (160 psi). The reaction mixture was then stirred (1200 rpm) for a further 0.5 h. To collect a series of data points, as in the case of Fig. 3, it should be noted that individual experiments were carried out and the reactant mixture was not sampled on-line.

### Degradation of H<sub>2</sub>O<sub>2</sub>

Catalytic activity towards H<sub>2</sub>O<sub>2</sub> degradation was determined in a similar manner to the direct synthesis activity of a catalyst. The autoclave liner was charged with solvent (methanol (5.6 g, HPLC grade, Fischer Scientific) and H<sub>2</sub>O (2.22 g, HPLC grade, Fischer Scientific)) and H<sub>2</sub>O<sub>2</sub> (50 wt% 0.68 g, Sigma Aldrich), with the solvent composition equivalent to a 4 wt% H<sub>2</sub>O<sub>2</sub> solution. From the solution, two 0.05 g aliquots were removed and titrated with acidified Ce(SO<sub>4</sub>)<sub>2</sub> solution using ferroin as an indicator to determine an accurate concentration of H<sub>2</sub>O<sub>2</sub> at the start of the reaction. Subsequently catalyst (0.01 g) was added to the reaction media and the autoclave was purged with 5% H<sub>2</sub>/CO<sub>2</sub> (100 psi) prior to being pressurised with 5% H<sub>2</sub>/CO<sub>2</sub> (420 psi). The reaction medium was conducted at a temperature of 20 °C and stirred at 1200 rpm for 0.5 h. After the reaction was complete the catalyst was removed from the reaction mixture and two 0.05 g aliquots were titrated against the acidified Ce(SO<sub>4</sub>)<sub>2</sub> solution using ferroin as an indicator. The degradation activity is reported as mol<sub>H<sub>2</sub>O<sub>2</sub></sub> kg<sub>cat</sub><sup>-1</sup> h<sup>-1</sup>.

### Catalyst reusability in the direct synthesis and degradation of H<sub>2</sub>O<sub>2</sub>

To determine catalyst reusability, a similar procedure to that outlined above for the direct synthesis of H<sub>2</sub>O<sub>2</sub> is followed utilising 0.05 g of catalyst. Following the initial test, the catalyst was recovered by filtration and dried (30 °C, 16 h, under vacuum); from the recovered catalyst sample 0.01 g was used to conduct a standard H<sub>2</sub>O<sub>2</sub> synthesis or degradation test.

**Note 3:** In all cases, the reactor temperature was controlled using a HAAKE K50 bath/circulator using an appropriate coolant.

**Note 4:** In all cases, reactions were run multiple times, over multiple batches of catalyst, with the data being presented as an average of these experiments.

### Characterisation

X-ray photoelectron spectroscopy (XPS) analyses were made on a Kratos Axis Ultra DLD spectrometer. Samples were mounted using double-sided adhesive tape and binding energies were referenced to the C(1s) binding energy of adventitious carbon contamination that was taken to be 284.8 eV. Monochromatic AlK<sub>α</sub> radiation was used for all measurements; an analyser pass energy of 160 eV was used for survey scans, while 40 eV was employed for more detailed regional scans. The intensities of the Au(4f), Pt(4f) and Pd(3d) features were used to derive the Pd/Pt and Au/Pt surface composition ratios.

Aberration-corrected scanning transmission electron microscopy (AC-STEM) was performed using a probe-corrected Hitachi HF5000 S/TEM, operating at 200 kV. The instrument was equipped with bright field (BF) and annular dark field (ADF) detectors for high spatial resolution STEM imaging experiments. This microscope was also equipped with dual Oxford Instruments XEDS detectors (2 × 100 mm<sup>2</sup>) having a total collection angle of 2.02 sr. Additional AC-STEM was performed using a probe-corrected ThermoFisher Scientific SPECTRA 200 operating at 200 kV and a JEOL ARM200F operating at 200 kV. In all cases, the samples were prepared by dry dispersion of the powder over 300 mesh holey carbon film copper grids.

Total metal leaching from the supported catalyst was quantified *via* inductively coupled plasma mass spectrometry (ICP-MS). Post-reaction solutions were analysed using an Agilent 7900 ICP-MS equipped with I-AS auto-sampler. All samples were diluted by a factor of 10 using HPLC grade H<sub>2</sub>O (1% HNO<sub>3</sub> and 0.5% HCl matrix). All calibrants were matrix-matched and measured against a five-point calibration using certified reference materials purchased from PerkinElmer and certified internal standards acquired from Agilent.

**Table 1** Catalytic activity of supported 0.5%PdAu/TiO<sub>2</sub> catalysts towards the direct synthesis and degradation of H<sub>2</sub>O<sub>2</sub>, as a function of Pd : Au ratio

Catalyst	Productivity/mol <sub>H<sub>2</sub>O<sub>2</sub></sub> kg <sub>cat</sub> <sup>-1</sup> h <sup>-1</sup>	H <sub>2</sub> O <sub>2</sub> Conc. / wt. %	H <sub>2</sub> Conv.%	H <sub>2</sub> O <sub>2</sub> Selectivity/%	Rate of reaction/mmol <sub>metal</sub> <sup>-1</sup> h <sup>-1</sup>	Degradation/mol <sub>H<sub>2</sub>O<sub>2</sub></sub> kg <sub>cat</sub> <sup>-1</sup> h <sup>-1</sup>
0.5%Pd/TiO <sub>2</sub>	68	0.140	57	44	1.49 × 10 <sup>3</sup>	0
0.375%Pd–0.125%Au/TiO <sub>2</sub>	80	0.170	61	50	2.02 × 10 <sup>3</sup>	110
0.25%Pd–0.25%Au/TiO <sub>2</sub>	90	0.180	53	59	2.49 × 10 <sup>3</sup>	119
0.125%Pd–0.375%Au/TiO <sub>2</sub>	74	0.150	40	76	2.43 × 10 <sup>3</sup>	108
0.5%Au/TiO <sub>2</sub>	3	0.010	BDL	BDL	1.06 × 10 <sup>2</sup>	0
0.25%Pd/TiO <sub>2</sub>	58	0.120	31	69	2.47 × 10 <sup>3</sup>	0
TiO <sub>2</sub> *	0	—	—	—	0	0

H<sub>2</sub>O<sub>2</sub> direct synthesis reaction conditions: catalyst (0.01 g), H<sub>2</sub>O (2.9 g), MeOH (5.6 g), 5% H<sub>2</sub>/CO<sub>2</sub> (420 psi), 25% O<sub>2</sub>/CO<sub>2</sub> (160 psi), 0.5 h, 20° C, 1200 rpm. H<sub>2</sub>O<sub>2</sub> degradation reaction conditions: catalyst (0.01 g), H<sub>2</sub>O<sub>2</sub> (50 wt% 0.68 g) H<sub>2</sub>O (2.22 g), MeOH (5.6 g), 5% H<sub>2</sub>/CO<sub>2</sub> (420 psi), 0.5 h, 20 °C 1200 rpm. BDL: below the accurate detection limit. \*TiO<sub>2</sub> used as received. Note: reaction rates are based on theoretical metal loading.



Brunauer–Emmett–Teller (BET) surface area measurements were conducted using a Quadrasorb surface area analyzer. A five-point isotherm of each material was measured using N<sub>2</sub> as the adsorbate gas. Samples were degassed at 250 °C for 2 h prior to the surface area being determined by five-point N<sub>2</sub> adsorption at –196 °C, and data were analyzed using the BET method.

## Results and discussion

Our initial studies investigated the efficacy of bimetallic PdAu and PdSn catalysts, prepared by a wet co-impregnation procedure, towards the direct synthesis and subsequent degradation of H<sub>2</sub>O<sub>2</sub> (Tables 1 and 2), under conditions considered detrimental towards the stability of the desired product, namely through the use of ambient reaction temperatures.<sup>37</sup> In keeping with a large body of literature<sup>20,21,26,39</sup> the alloying of Pd with Au resulted in a significant enhancement in H<sub>2</sub>O<sub>2</sub> synthesis activity (Table 1). Investigation of the role of Pd : Au ratio on catalytic performance, identified an optimal formulation of 0.25%Pd–0.25%Au/TiO<sub>2</sub>, with rates of H<sub>2</sub>O<sub>2</sub> synthesis (90 mol<sub>H<sub>2</sub>O<sub>2</sub></sub> kg<sub>cat</sub><sup>–1</sup> h<sup>–1</sup>), particularly noteworthy given the relatively low total metal loading utilised and the use of ambient reaction temperatures. Indeed the activity of the 0.25%Pd–0.25%Au/TiO<sub>2</sub> catalyst significantly exceeds that previously reported for analogous formulations consisting of ten times the total metal loading used in this study, when evaluated under conditions more conducive to H<sub>2</sub>O<sub>2</sub> stability.<sup>40</sup>

While the enhanced H<sub>2</sub>O<sub>2</sub> synthesis activity of the PdAu formulation, compared to the Pd-only analogue, may have been expected based on numerous previous studies, the inability of the 0.5%Pd/TiO<sub>2</sub> catalyst to degrade H<sub>2</sub>O<sub>2</sub> is perhaps surprising and may lead to the inference that this material is highly selective towards H<sub>2</sub>O<sub>2</sub>. However, it is important to note that the determination of H<sub>2</sub>O<sub>2</sub> selectivity under direct synthesis conditions contradicts this assumption. While the selectivity of the 0.25%Pd–0.25%Au/TiO<sub>2</sub> catalyst (59%) is significantly improved compared to the Pd-only analogue (44%), this metric is far from the total selectivity implied by our degradation studies. Notably, such selectivity comparisons were made at relatively similar rates of H<sub>2</sub> conversion (53 and 57% for the

0.25%Pd–0.25%Au/TiO<sub>2</sub> and 0.5%Pd/TiO<sub>2</sub> catalysts respectively). Such a discrepancy between H<sub>2</sub>O<sub>2</sub> degradation rates and H<sub>2</sub>O<sub>2</sub> selectivity, during H<sub>2</sub>O<sub>2</sub> synthesis, may be associated with the relatively high concentration of preformed oxidant used to conduct the H<sub>2</sub>O<sub>2</sub> degradation experiments (4 wt%), and the potential for metallic Pd species to be oxidised under such conditions. Indeed, the high H<sub>2</sub>O<sub>2</sub> selectivity of PdO, in comparison to Pd<sup>0</sup> species, has been well reported.<sup>41</sup> While the requirement to use such high concentrations of H<sub>2</sub>O<sub>2</sub> is evident, allowing for differences in catalytic activity to be more

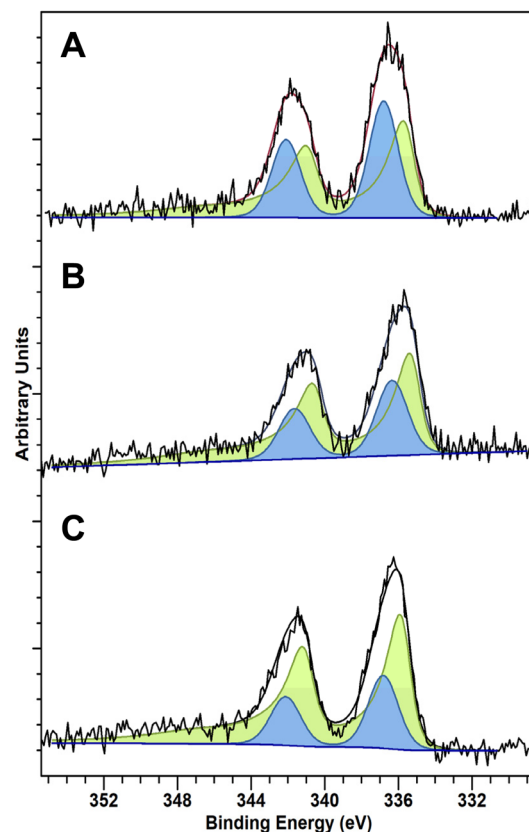


Fig. 1 XPS spectra of Pd(3d) regions of the as-prepared (A) 0.25%Pd–0.25%Sn/TiO<sub>2</sub>, (B) 0.25%Pd–0.25%Au/TiO<sub>2</sub> and (C) 0.5%Pd/TiO<sub>2</sub> catalysts. Key: Pd<sup>0</sup> (green) Pd<sup>2+</sup> (blue).

Table 2 Catalytic activity of supported 0.5%PdSn/TiO<sub>2</sub> catalysts towards the direct synthesis and degradation of H<sub>2</sub>O<sub>2</sub>, as a function of Pd : Sn ratio

Catalyst	Productivity/mol <sub>H<sub>2</sub>O<sub>2</sub></sub> kg <sub>cat</sub> <sup>–1</sup> h <sup>–1</sup>	H <sub>2</sub> O <sub>2</sub> Conc. / wt. %	H <sub>2</sub> Conv.%	H <sub>2</sub> O <sub>2</sub> selectivity/%	Rate of reaction/mmol <sub>metal</sub> <sup>–1</sup> h <sup>–1</sup>	Degradation/mol <sub>H<sub>2</sub>O<sub>2</sub></sub> kg <sub>cat</sub> <sup>–1</sup> h <sup>–1</sup>
0.5%Pd/TiO <sub>2</sub>	68	0.14	57	44	1.49 × 10 <sup>3</sup>	0
0.375%Pd–0.125%Sn/TiO <sub>2</sub>	64	0.13	46	50	1.40 × 10 <sup>3</sup>	0
0.25%Pd–0.25%Sn/TiO <sub>2</sub>	62	0.12	31	71	1.35 × 10 <sup>3</sup>	0
0.125%Pd–0.375%Sn/TiO <sub>2</sub>	22	0.08	16	89	9.23 × 10 <sup>2</sup>	0
0.5%Sn/TiO <sub>2</sub>	0	—	—	—	—	0
0.25%Pd/TiO <sub>2</sub>	58	0.12	31	69	2.47 × 10 <sup>3</sup>	0
TiO <sub>2</sub> *	0	—	—	—	0	0

H<sub>2</sub>O<sub>2</sub> direct synthesis reaction conditions: catalyst (0.01 g), H<sub>2</sub>O (2.9 g), MeOH (5.6 g), 5% H<sub>2</sub>/CO<sub>2</sub> (420 psi), 25% O<sub>2</sub>/CO<sub>2</sub> (160 psi), 0.5 h, 20 °C, 1200 rpm. H<sub>2</sub>O<sub>2</sub> degradation reaction conditions: catalyst (0.01 g), H<sub>2</sub>O<sub>2</sub> (50 wt% 0.68 g) H<sub>2</sub>O (2.22 g), MeOH (5.6 g), 5% H<sub>2</sub>/CO<sub>2</sub> (420 psi), 0.5 h, 20 °C 1200 rpm. \*TiO<sub>2</sub> used as received. Note: reaction rates are based on theoretical metal loading.



easily discerned, we consider that these observations highlight the need for the determination of  $\text{H}_2\text{O}_2$  selectivities under direct synthesis conditions in order to achieve a comprehensive understanding of catalytic performance.

By comparison to PdAu formulations, the application of PdSn based catalysts for the direct synthesis of  $\text{H}_2\text{O}_2$  has only recently begun to receive attention in the literature,<sup>27,31,33</sup> although it is

**Table 3** A comparison of initial  $\text{H}_2\text{O}_2$  synthesis rates over various  $\text{TiO}_2$  supported catalysts

Catalyst	Rate of reaction/ $\text{mmol}_{\text{H}_2\text{O}_2}$ $\text{mmol}_{\text{metal}}^{-1} \text{h}^{-1}$	
	5 min	30 min
0.5%Pd/ $\text{TiO}_2$	$4.21 \times 10^3$	$1.49 \times 10^3$
0.25%Pd–0.25%Au/ $\text{TiO}_2$	$5.87 \times 10^3$	$2.49 \times 10^3$
0.25%Pd–0.25%Sn/ $\text{TiO}_2$	$5.21 \times 10^3$	$1.35 \times 10^3$

$\text{H}_2\text{O}_2$  direct synthesis reaction conditions: catalyst (0.01 g),  $\text{H}_2\text{O}$  (2.9 g), MeOH (5.6 g), 5%  $\text{H}_2/\text{CO}_2$  (420 psi), 25%  $\text{O}_2/\text{CO}_2$  (160 psi), 20 °C 1200 rpm. Note: reaction rates are based on theoretical metal loading.

clear that such catalysts can rival the performance of *state-of-the-art* materials.<sup>27</sup> Investigation into the Pd : Sn ratio revealed that, unlike the PdAu system, the introduction of small quantities of the secondary metal did not significantly improve catalytic performance compared to the 0.5%Pd/ $\text{TiO}_2$  catalyst ( $68 \text{ mol}_{\text{H}_2\text{O}_2} \text{ kg}_{\text{cat}}^{-1} \text{ h}^{-1}$ ) (Table 2). A comparison of the 0.25%Pd/ $\text{TiO}_2$  and 0.25%Pd–0.25%Sn/ $\text{TiO}_2$  catalysts (*i.e.* formulations with an equivalent Pd loading), further indicates that the introduction of low concentrations of Sn does not result in a meaningful enhancement in catalytic performance, compared to Pd-analogues. Indeed, the performance of the 0.25%Pd/ $\text{TiO}_2$  ( $58 \text{ mol}_{\text{H}_2\text{O}_2} \text{ kg}_{\text{cat}}^{-1} \text{ h}^{-1}$  and 69%  $\text{H}_2\text{O}_2$  selectivity) and 0.25%Pd–0.25%Sn/ $\text{TiO}_2$  ( $62 \text{ mol}_{\text{H}_2\text{O}_2} \text{ kg}_{\text{cat}}^{-1} \text{ h}^{-1}$  and 71%  $\text{H}_2\text{O}_2$  selectivity) catalysts were found to be nearly identical.

We were subsequently motivated to investigate a subset of catalyst formulations, namely the 0.5%Pd/ $\text{TiO}_2$ , 0.25%Pd–0.25%Au/ $\text{TiO}_2$  and 0.25%Pd–0.25%Sn/ $\text{TiO}_2$  catalysts, in order to gain further insight into these materials.

The activity of Pd-based catalysts towards  $\text{H}_2\text{O}_2$  production is well known to be highly influenced by Pd oxidation state. In particular, the presence of PdO has been reported to aid the

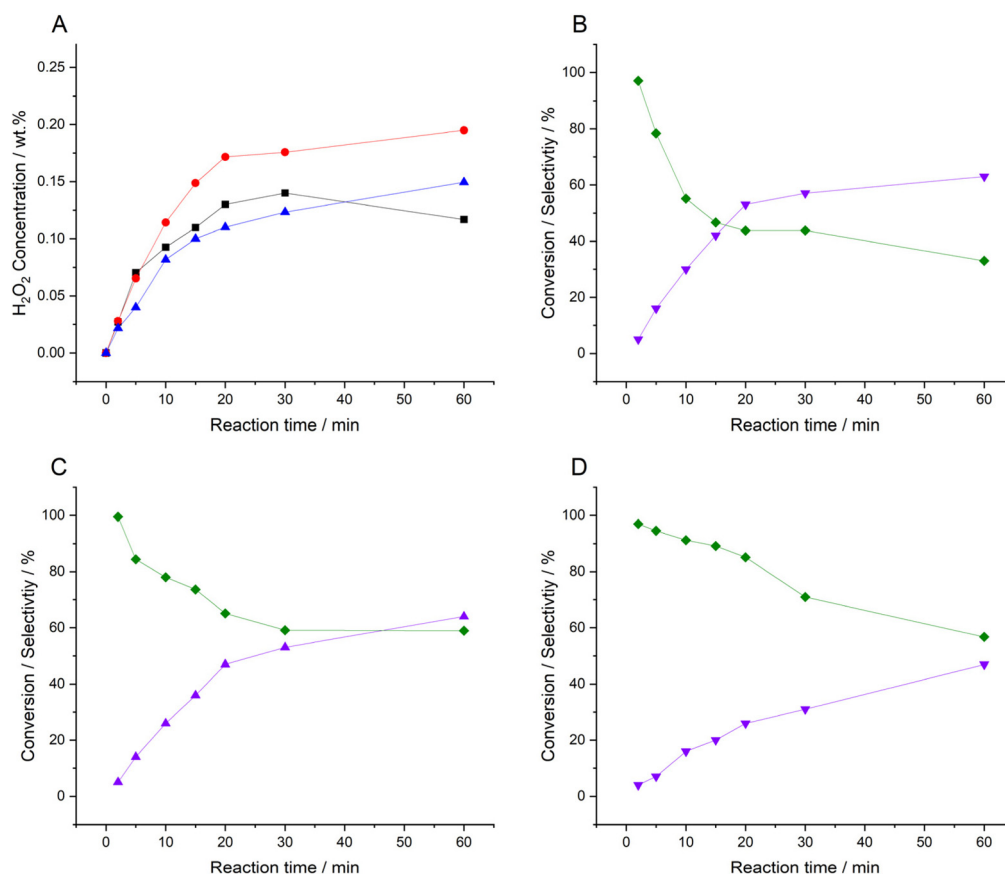


**Fig. 2** Comparison of catalytic activity towards the direct synthesis of  $\text{H}_2\text{O}_2$ , as a function of reaction time. (A) Catalytic activity based on net  $\text{H}_2\text{O}_2$  concentration. Determination of  $\text{H}_2$  conversion and  $\text{H}_2\text{O}_2$  selectivity for the (B) 0.5%Pd/ $\text{TiO}_2$  (C) 0.25%Pd–0.25%Au/ $\text{TiO}_2$  and (D) 0.25%Pd–0.25%Sn/ $\text{TiO}_2$  catalysts Key: 0.5%Pd/ $\text{TiO}_2$  (black squares), 0.25%Pd–0.25%Au/ $\text{TiO}_2$  (red circles), 0.25%Pd–0.25%Sn/ $\text{TiO}_2$  catalysts (blue triangles)  $\text{H}_2$  conversion (purple inverted triangles),  $\text{H}_2\text{O}_2$  selectivity (green diamonds).  $\text{H}_2\text{O}_2$  direct synthesis reaction conditions: catalyst (0.01 g),  $\text{H}_2\text{O}$  (2.9 g), MeOH (5.6 g), 5%  $\text{H}_2/\text{CO}_2$  (420 psi), 25%  $\text{O}_2/\text{CO}_2$  (160 psi), 20 °C, 1200 rpm.



suppression of O–O bond dissociation and the unselective formation of H<sub>2</sub>O, in addition to promoting the rapid desorption of H<sub>2</sub>O<sub>2</sub> from catalytic surfaces, with both factors resulting in improved catalytic selectivity.<sup>42</sup> While the identity of the true active site for H<sub>2</sub>O<sub>2</sub> synthesis is still debated, there is a consensus that a proportion of the Pd must exist in the reduced state to form H<sub>2</sub>O<sub>2</sub>. However, it is not clear if the active sites that bind and selectively reduce O<sub>2</sub> to H<sub>2</sub>O<sub>2</sub> are fully or partially reduced or indeed fully oxidized Pd atoms, for a detailed discussion of this we direct the reader to the excellent review on the topic by D.W. Flaherty.<sup>14</sup> Analysis of the as-prepared materials by X-ray photoelectron spectroscopy (XPS) is reported in Fig. 1 and reveals clear differences in Pd speciation across the catalytic series. Despite exposure to a high-temperature oxidative heat treatment (static air, 400 °C, 3 h, 10 °C min<sup>-1</sup>), all catalysts were found to consist of mixed Pd oxidation states (*i.e.* Pd<sup>2+</sup> and Pd<sup>0</sup>). However, the introduction of Au and Sn was found to significantly shift Pd speciation towards Pd<sup>2+</sup>. Notably, our observations align well with earlier works which have identified the ability of both metals to modify the electronic state of Pd which, at least in the case of the PdAu cata-

lyst, may be partly responsible for the improved catalytic activity, when compared to the Pd-only analogue.<sup>33,43</sup> Although it should be noted that the Pd oxidation state of the as-prepared materials may not be fully representative of that under reaction conditions.

A comparison of the initial rate of reaction, determined at a reaction time of 5 minutes, where the contribution of competitive H<sub>2</sub>O<sub>2</sub> degradation pathways can be considered to be negligible, is reported in Table 3 and further reveals the enhanced activity of the 0.25%Pd–0.25%Au/TiO<sub>2</sub> catalyst.

Time-on-line studies comparing H<sub>2</sub>O<sub>2</sub> synthesis rates over the catalytic series are reported in Fig. 2. The enhanced activity of the 0.25%Pd–0.25%Au/TiO<sub>2</sub> catalyst is again apparent, particularly at extended reaction times, with the concentration of H<sub>2</sub>O<sub>2</sub> (0.21 wt%) significantly greater than that achieved by either the 0.25%Pd–0.25%Sn/TiO<sub>2</sub> (0.15 wt%) or 0.5%Pd/TiO<sub>2</sub> (0.12 wt%) analogues. Comparison of catalytic selectivity towards H<sub>2</sub>O<sub>2</sub>, at near iso-conversion further identifies the greater efficacy of the PdAu formulation, particularly at relatively high rates of H<sub>2</sub> conversion (Table S.2†). However, the improved selectivity of the 0.25%Pd–0.25%Sn/TiO<sub>2</sub> catalyst (91%) at relatively low rates of H<sub>2</sub> conversion (approx. 15%), is notable, outperforming both the 0.25%Pd–0.25%Au/TiO<sub>2</sub> (83% selectivity at 14% H<sub>2</sub> conversion) and 0.5%Pd/TiO<sub>2</sub> (78% selectivity at 16% H<sub>2</sub> conversion) analogues. Assessment of the catalysts by XPS, over the course of the H<sub>2</sub>O<sub>2</sub> synthesis reaction, reveals a clear shift in Pd oxidation state, towards Pd<sup>0</sup>, which may be expected given the reductive atmosphere used and correlates well with the observed loss of selectivity over all three formulations on-stream, with the lower selectivity of Pd<sup>0</sup> towards H<sub>2</sub>O<sub>2</sub>, compared to Pd<sup>2+</sup> species well reported (Fig. S.1†).<sup>44</sup> Notably, in the case of the 0.25%Pd–0.25%Sn/TiO<sub>2</sub> catalyst our XPS analysis reveals a significant reduction of Pd<sup>2+</sup> at extended reaction times (Fig. S.1†), which aligns well with the observed loss of selectivity.

Evaluation of catalytic performance over successive H<sub>2</sub>O<sub>2</sub> synthesis experiments, where the gaseous reagents were replenished at 30-minute intervals, was subsequently conducted (Fig. 3). After five consecutive H<sub>2</sub>O<sub>2</sub> reactions the improved performance of the 0.25%Pd–0.25%Au/TiO<sub>2</sub> catalyst is again clear (0.52 wt%). However, based on catalytic activity measurements over our standard reaction time (0.5 h), one may not have expected the relatively high H<sub>2</sub>O<sub>2</sub> concentration

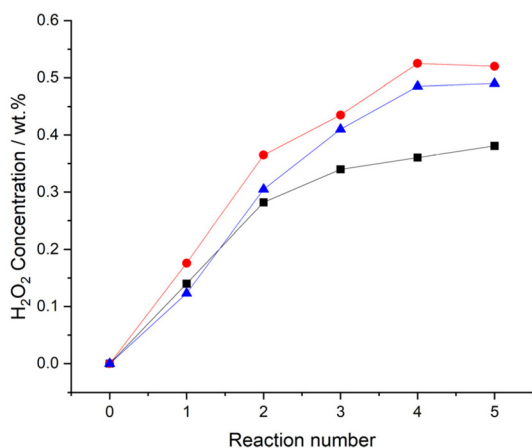


**Fig. 3** Comparison of catalytic activity, over sequential H<sub>2</sub>O<sub>2</sub> synthesis reactions. Key: 0.5%Pd/TiO<sub>2</sub> (black squares), 0.25%Pd–0.25%Au/TiO<sub>2</sub> (red circles), 0.25%Pd–0.25%Sn/TiO<sub>2</sub> catalysts (blue triangles) H<sub>2</sub>O<sub>2</sub> direct synthesis reaction conditions: catalyst (0.01 g), H<sub>2</sub>O (2.9 g), MeOH (5.6 g), 5% H<sub>2</sub>/CO<sub>2</sub> (420 psi), 25% O<sub>2</sub>/CO<sub>2</sub> (160 psi), 0.5 h, 20 °C, 1200 rpm.

**Table 4** Catalyst re-usability towards the direct synthesis and subsequent degradation of H<sub>2</sub>O<sub>2</sub>

Catalyst	Productivity/ mol <sub>H<sub>2</sub>O<sub>2</sub></sub> kg <sub>cat</sub> <sup>-1</sup> h <sup>-1</sup>		H <sub>2</sub> Conv. /%		H <sub>2</sub> O <sub>2</sub> selectivity/ %		Degradation/ mol <sub>H<sub>2</sub>O<sub>2</sub></sub> kg <sub>cat</sub> <sup>-1</sup> h <sup>-1</sup>		Metal leaching/%		
	Use 1	Use 2	Use 1	Use 2	Use 1	Use 2	Use 1	Use 2	Pd	Au	Sn
0.5%Pd/TiO <sub>2</sub>	68	44	57	62	44	25	0	321	1.90	—	—
0.25%Pd–0.25%Au/TiO <sub>2</sub>	90	53	53	60	59	32	100	148	1.57	0	—
0.25%Pd–0.25%Sn/TiO <sub>2</sub>	62	34	31	39	71	30	0	88	1.45	—	1.26

H<sub>2</sub>O<sub>2</sub> direct synthesis reaction conditions: catalyst (0.01 g), H<sub>2</sub>O (2.9 g), MeOH (5.6 g), 5% H<sub>2</sub>/CO<sub>2</sub> (420 psi), 25% O<sub>2</sub>/CO<sub>2</sub> (160 psi), 0.5 h, 20 °C, 1200 rpm.



achieved by the 0.25%Pd–0.25%Sn/TiO<sub>2</sub> catalyst (0.49 wt%). Indeed, the similar performance of the two bimetallic catalysts is striking, with both catalysts achieving concentrations of H<sub>2</sub>O<sub>2</sub> comparable to that we have previously reported using a near 100% selective 3%Pd–2%Sn/TiO<sub>2</sub> catalyst,<sup>27</sup> this is despite the less conducive reaction conditions and signifi-

cantly lower active metals loading of the catalysts reported within this work.

With the requirement to successfully reuse a catalyst at the heart of green chemistry, we next evaluated catalytic activity towards H<sub>2</sub>O<sub>2</sub> synthesis and H<sub>2</sub>O<sub>2</sub> degradation pathways, upon re-use (Table 4). It was found that for all formulations studied,

**Table 5** The effect of secondary metal loading on the activity of the 0.25%Pd/TiO<sub>2</sub> catalyst towards the direct synthesis and subsequent degradation of H<sub>2</sub>O<sub>2</sub>

Catalyst	Productivity/mol <sub>H<sub>2</sub>O<sub>2</sub></sub> kg <sub>cat</sub> <sup>-1</sup> h <sup>-1</sup>	H <sub>2</sub> O <sub>2</sub> Conc. / wt. %	H <sub>2</sub> Conv.%	H <sub>2</sub> O <sub>2</sub> selectivity/%	Rate of reaction/mmol <sub>H<sub>2</sub>O<sub>2</sub></sub> mmol <sub>metal</sub> <sup>-1</sup> h <sup>-1</sup>	Degradation/mol <sub>H<sub>2</sub>O<sub>2</sub></sub> kg <sub>cat</sub> <sup>-1</sup> h <sup>-1</sup>
0.25%Pd/TiO <sub>2</sub>	58	0.120	31	69	2.55 × 10 <sup>3</sup>	0
0.25%Pd–0.25%Au/TiO <sub>2</sub>	90	0.180	53	59	2.71 × 10 <sup>3</sup>	119
0.25%Pd–0.5%Au/TiO <sub>2</sub>	70	0.140	38	65	1.42 × 10 <sup>3</sup>	90
0.25%Pd–0.75%Au/TiO <sub>2</sub>	65	0.130	33	70	1.05 × 10 <sup>3</sup>	79
0.25%Pd–1.5%Au/TiO <sub>2</sub>	52	0.110	24	78	5.26 × 10 <sup>2</sup>	40
0.25%Pd–2.25%Au/TiO <sub>2</sub>	44	0.080	18	83	3.05 × 10 <sup>2</sup>	6
0.25%Pd–0.25%Sn/TiO <sub>2</sub>	62	0.120	31	71	1.35 × 10 <sup>3</sup>	0
0.25%Pd–0.5% Sn /TiO <sub>2</sub>	75	0.150	31	84	1.11 × 10 <sup>3</sup>	0
0.25%Pd–0.75% Sn /TiO <sub>2</sub>	83	0.160	32	90	9.22 × 10 <sup>2</sup>	0
0.25%Pd–1.5% Sn/TiO <sub>2</sub>	88	0.180	34	93	5.93 × 10 <sup>2</sup>	0
0.25%Pd–2.25% Sn /TiO <sub>2</sub>	92	0.185	35	94	4.34 × 10 <sup>2</sup>	0

H<sub>2</sub>O<sub>2</sub> direct synthesis reaction conditions: catalyst (0.01 g), H<sub>2</sub>O (2.9 g), MeOH (5.6 g), 5% H<sub>2</sub>/CO<sub>2</sub> (420 psi), 25% O<sub>2</sub>/CO<sub>2</sub> (160 psi), 0.5 h, 20° C, 1200 rpm. H<sub>2</sub>O<sub>2</sub> degradation reaction conditions: catalyst (0.01 g), H<sub>2</sub>O<sub>2</sub> (50 wt% 0.68 g) H<sub>2</sub>O (2.22 g), MeOH (5.6 g), 5% H<sub>2</sub>/CO<sub>2</sub> (420 psi), 0.5 h, 20° C 1200 rpm.

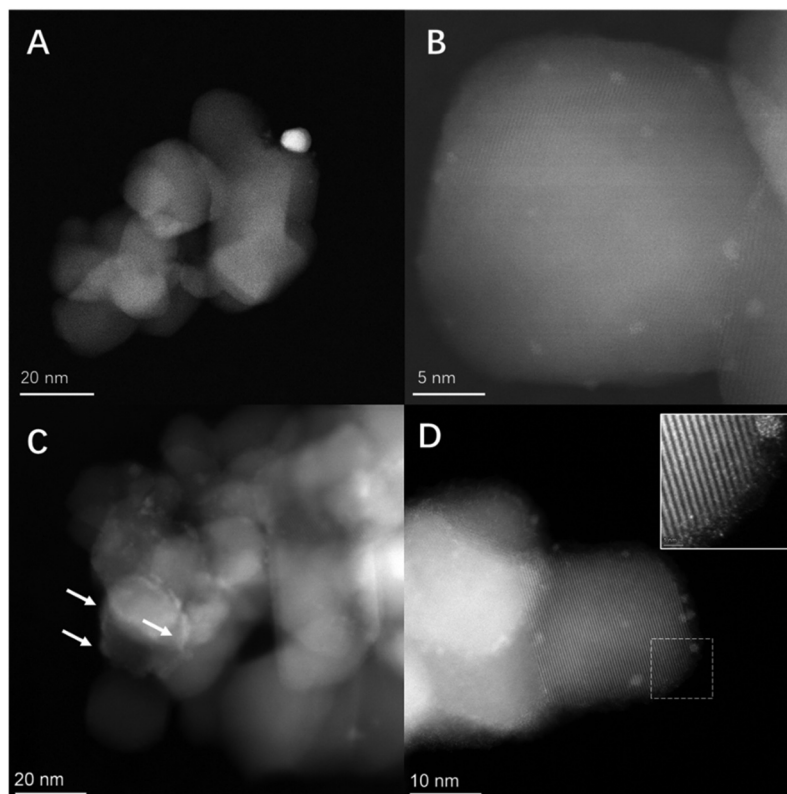


**Fig. 4** Aberration corrected STEM images of 0.25%Pd–0.25%Au/TiO<sub>2</sub> and 0.25%Pd–2.25%Sn/TiO<sub>2</sub> catalysts. (A) HAADF image of the 0.25%Pd–0.25%Au/TiO<sub>2</sub> catalyst showing larger Au–Pd alloyed particles and (B) HAADF image of the 0.25%Pd–0.25%Au/TiO<sub>2</sub> catalyst showing smaller <1 nm Pd-rich clusters. (C) HAADF image of the 0.25%Pd–2.25%Sn/TiO<sub>2</sub> catalyst showing islands of SnO<sub>x</sub> over the TiO<sub>2</sub> support surface and (D) HAADF image of 0.25%Pd–2.25%Sn/TiO<sub>2</sub> showing smaller <3 nm Pd particles along with (inset) magnified image of highlighted area showing atomically dispersed Pd. Note: In all cases, active metallic species are identified by high Z-contrast (*i.e.* brighter regions of the micrograph).



catalytic activity towards  $\text{H}_2\text{O}_2$  production decreased considerably upon second use. Determination of metal leaching during the direct synthesis reaction *via* ICP-MS analysis of post-reaction solutions is also reported in Table 4, a degree of metal leaching was observed for all catalysts, although we should highlight no Au leaching was detected, and in all cases the degree of metal leaching is relatively low (<2%). As such it is considered that the loss in catalytic performance upon reuse does not result from the leaching of active metals. Rather, we consider that changes in catalytic selectivity explain the observed variation in catalytic performance between first and second use. For all catalysts studied,  $\text{H}_2\text{O}_2$  degradation rates were found to increase considerably upon reuse. This is particularly noteworthy for the 0.5%Pd/TiO<sub>2</sub> (321 mol<sub>H<sub>2</sub>O<sub>2</sub></sub> kg<sub>cat</sub><sup>-1</sup> h<sup>-1</sup>) and 0.25%Pd–0.25%Sn/TiO<sub>2</sub> (88 mol<sub>H<sub>2</sub>O<sub>2</sub></sub> kg<sub>cat</sub><sup>-1</sup> h<sup>-1</sup>) catalysts given that neither offered any activity towards  $\text{H}_2\text{O}_2$  degradation upon initial use (Tables 1 and 2). Our analysis of the catalysts after use in the direct synthesis of  $\text{H}_2\text{O}_2$  *via* XPS (Fig. S.2†) revealed a clear shift towards Pd<sup>0</sup> for all formulations. With the enhanced activity of Pd<sup>0</sup> species towards  $\text{H}_2\text{O}_2$  degradation well known<sup>44</sup> it is possible to, at least in part, attribute the decreased  $\text{H}_2\text{O}_2$  selectivity of these catalysts to the *in situ* reduction of Pd<sup>2+</sup> to Pd<sup>0</sup> species.

We have previously demonstrated that the introduction of large quantities of base metals (including Sn, Ni, Ga, In, Zn and Co) into a supported Pd catalyst can significantly improve

catalyst performance towards  $\text{H}_2\text{O}_2$  production.<sup>27,28</sup> Notably, while all formulations were found to be highly selective towards  $\text{H}_2\text{O}_2$ , the reactivity of the optimal PdSn catalyst was two to three times greater than analogous materials containing alternative transition metals.<sup>27</sup> Motivated by these earlier works we subsequently investigated the effect of varying Au and Sn loading on catalytic reactivity and selectivity, while maintaining Pd content at 0.25 wt% (Table 5).

As discussed above, the introduction of relatively small quantities of Au (Pd:Au = 1 (wt/wt)), led to a considerable increase in the rate of  $\text{H}_2\text{O}_2$  production (90 mol<sub>H<sub>2</sub>O<sub>2</sub></sub> kg<sub>cat</sub><sup>-1</sup> h<sup>-1</sup>). However, increasing Au content further resulted in a significant loss in catalytic performance, with the activity of the 0.25%Pd–2.25%Au/TiO<sub>2</sub> catalyst (44 mol<sub>H<sub>2</sub>O<sub>2</sub></sub> kg<sub>cat</sub><sup>-1</sup> h<sup>-1</sup> and 18%  $\text{H}_2$  conversion) less than half that observed over the optimal 0.25%Pd–0.25%Au/TiO<sub>2</sub> formulation (90 mol<sub>H<sub>2</sub>O<sub>2</sub></sub> kg<sub>cat</sub><sup>-1</sup> h<sup>-1</sup> and 53%  $\text{H}_2$  conversion). In contrast to the PdAu system, the introduction of high loadings of Sn was found to significantly enhance catalytic activity, with the  $\text{H}_2\text{O}_2$  synthesis rate of the 0.25%Pd–2.25%Sn/TiO<sub>2</sub> catalyst (92 mol<sub>H<sub>2</sub>O<sub>2</sub></sub> kg<sub>cat</sub><sup>-1</sup> h<sup>-1</sup>) 1.6 times greater than the 0.25%Pd/TiO<sub>2</sub> analogue (58 mol<sub>H<sub>2</sub>O<sub>2</sub></sub> kg<sub>cat</sub><sup>-1</sup> h<sup>-1</sup>) and comparable to that offered by the optimal 0.25%Pd–0.25%Au/TiO<sub>2</sub> formulation (90 mol<sub>H<sub>2</sub>O<sub>2</sub></sub> kg<sub>cat</sub><sup>-1</sup> h<sup>-1</sup>). Notably, we did not extend our study beyond a Pd:Sn ratio of 1:10 and so further improvements may be obtained through further optimisation of metal loading.

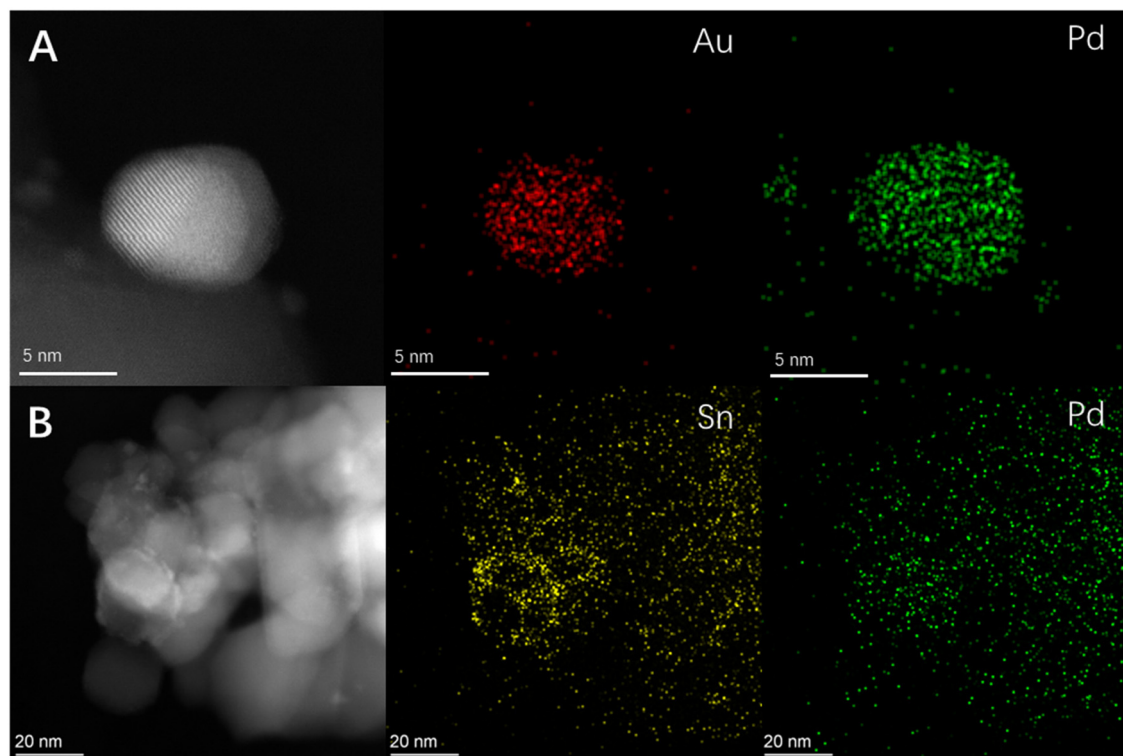


**Fig. 5** HAADF-STEM and XEDS maps of (A) 0.25%Pd–0.25%Au/TiO<sub>2</sub> showing the formation of AuPd alloys in the larger particles and (B) 0.25%Pd–2.25%Sn/TiO<sub>2</sub> showing the presence of SnO<sub>x</sub> islands and well dispersed Pd species. Note: In all cases, active metallic species are identified by high Z-contrast (*i.e.* brighter regions of the micrograph).





Interestingly, the observed catalytic improvement upon the introduction of high concentrations of Sn was found to result from an increase in the selective utilisation of H<sub>2</sub>, rather than an increase in the rate of H<sub>2</sub>O<sub>2</sub> production, as indicated by H<sub>2</sub> conversion measurements, with this metric varying little across the catalytic series. Indeed, the H<sub>2</sub>O<sub>2</sub> selectivity of the 0.25%Pd–2.25%Sn/TiO<sub>2</sub> catalyst (94%), was found to be comparable to that offered by *state-of-the-art* formulations.

Focussing on the 0.25%Pd–2.25%Sn/TiO<sub>2</sub> catalyst and in an attempt to improve the net concentration of H<sub>2</sub>O<sub>2</sub>, we conducted a series of sequential H<sub>2</sub>O<sub>2</sub> direct synthesis experiments (Fig. S.3†). After five consecutive reactions, the net concentration of H<sub>2</sub>O<sub>2</sub> increased to a value of 0.69 wt%, which is far superior to the yields of H<sub>2</sub>O<sub>2</sub> achieved over the 0.5%Pd/TiO<sub>2</sub> (0.38 wt% H<sub>2</sub>O<sub>2</sub>), 0.25%Pd–0.25%Au/TiO<sub>2</sub> (0.52 wt% H<sub>2</sub>O<sub>2</sub>) or 0.25%Pd–0.25%Sn/TiO<sub>2</sub> (0.49 wt% H<sub>2</sub>O<sub>2</sub>) catalysts over the same number of reactions (Fig. 3).

HAADF/ADF-STEM (Fig. 4) and corresponding EDX (Fig. 5) analysis of optimal PdAu and PdSn formulations (*i.e.* the 0.25%Pd–0.25%Au/TiO<sub>2</sub> and 0.25%Pd–2.25%Sn/TiO<sub>2</sub> catalysts), in addition to the parent 0.25%Pd/TiO<sub>2</sub> catalyst (Fig. S.4†), was conducted in order to gain further insight into underlying cause for the promotive effect observed through secondary metal introduction. A considerable variation in nanoparticle size across the catalytic series was observed. Perhaps as expected given the low metal loading of the 0.25%Pd/TiO<sub>2</sub> catalyst Pd was found to be present primarily as sub-nanometre clusters, with a very limited number of nanoparticles in the 3–5 nm range also observed (Fig. S.4†). The alloying of Pd with Au resulted in the bifurcation of particle size, with a proportion of larger (10–15 nm) nanoparticles observed in addition to smaller clusters (Fig. 4A and B). Subsequent STEM-XEDS mapping of individual nanoparticles, as presented in Fig. 5A, confirmed that the larger particles consisted of random alloys of Pd and Au, while the smaller clusters were found to consist of a mixture of Pd-only and AuPd alloys (Fig. S.5†), which is in keeping with our previous investigations into similar materials.<sup>45</sup> By comparison the introduction of large quantities of Sn resulted in an improved dispersion of Pd and the formation of single atoms of Pd, surrounded by Sn/SnO<sub>x</sub> domains (Fig. 4C and D, with additional data reported in Fig. S.6†). Notably, our analysis of the PdSn catalytic series by XPS (Fig. S.7†) indicated that, regardless of Sn content, Pd speciation remained broadly similar for all formulations. As such, it is possible to conclude that the improved catalytic performance of the 0.25%Pd–2.25%Sn/TiO<sub>2</sub> catalyst is not a result of the electronic modification of Pd species. Rather, we consider that the primary cause for the enhanced activity is a result of the improved dispersion of Pd species with the introduction of Sn. Such observations would align well with the numerous studies that have demonstrated the dependency of catalytic performance on nanoparticle size, and that in particular highly dispersed Pd species can offer exceptional selectivity towards H<sub>2</sub>O<sub>2</sub>.<sup>46–48</sup>

## Conclusions

The efficacy of a series of PdAu and PdSn catalysts prepared by a wet co-impregnation methodology for the direct synthesis of H<sub>2</sub>O<sub>2</sub> has been compared, with the introduction of both Au and Sn into supported Pd nanoparticles found to result in an improved catalytic performance. While the introduction of relatively low concentrations of Au resulted in a considerable synergistic enhancement in catalyst activity (Pd : Au = 1 : 1 (wt/wt)), significantly larger Sn loadings were required to rival the H<sub>2</sub>O<sub>2</sub> synthesis rates offered by the optimal PdAu formulation (Pd : Sn = 1 : 10 (wt/wt)). A 0.25%Pd–2.25%Sn/TiO<sub>2</sub> catalyst was found to be highly selective towards H<sub>2</sub>O<sub>2</sub>, with this metric comparable to that offered by *state-of-the-art* materials, due to improved Pd dispersion. While we consider that these catalysts represent a promising basis for further exploration, additional efforts are required to improve catalyst stability if they are to fully rival leading formulations.

## Author contributions

D. K. and R. J. L. conducted catalytic synthesis, testing and data analysis. D. K., R. J. L., C. C., D. J. M., T. E. D, A. L., T. Q., C. S. A. and X. L. conducted catalyst characterisation and corresponding data processing. R. J. L. and G. J. H. contributed to the design of the study. R. J. L., A. L., J. K. E., L. C., M. S. R., X. L. and G. J. H. provided technical advice and result interpretation. R. J. L. wrote the manuscript and ESI with all authors commenting on and amending both documents. All authors discussed and contributed to the work.

## Conflicts of interest

The authors declare no conflicts of interest.

## Acknowledgements

The authors wish to thank the financial support and detailed discussion with Haldor Topsøe.

Additionally, the Cardiff University electron microscope facility (CCI-EMF) and Diamond Light Source electron Physical Science Imaging Centre (ePSIC proposal number MG27777) is acknowledged for the transmission electron microscopy. XPS data collection was performed at the EPSRC National Facility for XPS ('HarwellXPS'), operated by Cardiff University and University College London, under contract No. PR16195. D. K. and C. C. acknowledge Haldor Topsøe for financial support. R. J. L. and G. J. H. gratefully acknowledge the Max Planck Centre for Fundamental Heterogeneous Catalysis (FUNCAT) for financial support. X. L. acknowledges financial support from National Key R&D Program of China (2021YFA1500300 and 2022YFA1500146) and National Natural Science Foundation of China (22072090 and 22272106). L. C.



acknowledges the financial support from National Natural Science Foundation of China (21991153 and 21991150).

## References

- S. H. Zeronian and M. K. Inglesby, *Cellulose*, 1995, **2**, 265–272.
- V. Russo, R. Tesser, E. Santacesaria and M. Di Serio, *Ind. Eng. Chem. Res.*, 2013, **52**, 1168–1178.
- M. Lin, C. Xia, B. Zhu, H. Li and X. Shu, *Chem. Eng. J.*, 2016, **295**, 370–375.
- C. M. Crombie, R. J. Lewis, D. Kovačič, D. J. Morgan, T. J. A. Slater, T. E. Davies, J. K. Edwards, M. S. Skjøth-Rasmussen and G. J. Hutchings, *Catal. Lett.*, 2021, **151**, 2762–2774.
- Y. Du, Y. Xiong, J. Li and X. Yang, *J. Mol. Catal. A: Chem.*, 2009, **298**, 12–16.
- G. Goor, J. Glenneberg, S. Jacobi, J. Dadabhoy and E. Candido, *Ullmann's Encyclopedia of Industrial Chemistry*, 2019.
- J. R. Scoville and I. A. Novicova, *US 5900256*, 1996, Cottrell Ltd.
- G. Gao, Y. Tian, X. Gong, Z. Pan, K. Yang and B. Zong, *Chin. J. Catal.*, 2020, **41**, 1039–1047.
- R. J. Lewis and G. J. Hutchings, *ChemCatChem*, 2019, **11**, 298–308.
- J. M. Campos-Martin, G. Blanco-Brieva and J. L. G. Fierro, *Angew. Chem., Int. Ed.*, 2006, **45**, 6962–6984.
- R. J. Lewis, K. Ueura, X. Liu, Y. Fukuta, T. Qin, T. E. Davies, D. J. Morgan, A. Stenner, J. Singleton, J. K. Edwards, S. J. Freakley, C. J. Kiely, L. Chen, Y. Yamamoto and G. J. Hutchings, *ACS Catal.*, 2023, **13**, 1934–1945.
- C. M. Crombie, R. J. Lewis, R. L. Taylor, D. J. Morgan, T. E. Davies, A. Folli, D. M. Murphy, J. K. Edwards, J. Qi, H. Jiang, C. J. Kiely, X. Liu, M. S. Skjøth-Rasmussen and G. J. Hutchings, *ACS Catal.*, 2021, **11**, 2701–2714.
- Z. Jin, L. Wang, E. Zuidema, K. Mondal, M. Zhang, J. Zhang, C. Wang, X. Meng, H. Yang, C. Mesters and F. Xiao, *Science*, 2020, **367**, 193–197.
- D. W. Flaherty, *ACS Catal.*, 2018, **8**, 1520–1527.
- R. J. Lewis, E. N. Ntainjua, D. J. Morgan, T. E. Davies, A. F. Carley, S. J. Freakley and G. J. Hutchings, *Catal. Commun.*, 2021, **161**, 106358.
- G. Gallina, J. García-Serna, T. O. Salmi, P. Canu and P. Biasi, *Ind. Eng. Chem. Res.*, 2017, **56**, 13367–13378.
- Y. Han and J. H. Lunsford, *J. Catal.*, 2005, **230**, 313–316.
- Q. Liu, J. C. Bauer, R. E. Schaak and J. H. Lunsford, *Appl. Catal., A*, 2008, **339**, 130–136.
- P. Priyadarshini, T. Ricciardulli, J. S. Adams, Y. S. Yun and D. W. Flaherty, *J. Catal.*, 2021, **399**, 24–40.
- J. K. Edwards, B. Solsona, E. N. Ntainjua, A. F. Carley, A. A. Herzing, C. J. Kiely and G. J. Hutchings, *Science*, 2009, **323**, 1037–1041.
- T. Ricciardulli, S. Gorthy, J. S. Adams, C. Thompson, A. M. Karim, M. Neurock and D. W. Flaherty, *J. Am. Chem. Soc.*, 2021, **143**, 5445–5464.
- M. Kim, G.-H. Han, X. Xiao, J. Song, J. Hong, E. Jung, H. Kim, J. Ahn, S. S. Han, K. Lee and T. Yu, *Appl. Surf. Sci.*, 2021, **562**, 150031.
- Y. Zhang, Q. Sun, G. Guo, Y. Cheng, X. Zhang, H. Ji and X. He, *Chem. Eng. J.*, 2023, **451**, 138867.
- G. Han, X. Xiao, J. Hong, K. Lee, S. Park, J. Ahn, K. Lee and T. Yu, *ACS Appl. Mater. Interfaces*, 2020, **12**, 6328–6335.
- N. M. Wilson, P. Priyadarshini, S. Kunz and D. W. Flaherty, *J. Catal.*, 2018, **357**, 163–175.
- J. Li, T. Ishihara and K. Yoshizawa, *J. Phys. Chem. C*, 2011, **115**, 25359–25367.
- S. J. Freakley, Q. He, J. H. Harrhy, L. Lu, D. A. Crole, D. J. Morgan, E. N. Ntainjua, J. K. Edwards, A. F. Carley, A. Y. Borisevich, C. J. Kiely and G. J. Hutchings, *Science*, 2016, **351**, 965–968.
- D. A. Crole, R. Underhill, J. K. Edwards, G. Shaw, S. J. Freakley, G. J. Hutchings and R. J. Lewis, *Philos. Trans. R. Soc., A*, 2020, **378**, 20200062.
- H. Xu, D. Cheng and Y. Gao, *ACS Catal.*, 2017, **7**, 2164–2170.
- Y. Wang, H. Pan, Q. Lin, Y. Shi and J. Zhang, *Catalysts*, 2020, **10**, 303.
- Z. Yang, Z. Hao, S. Zhou, P. Xie, Z. Wei, S. Zhao and F. Gong, *ACS Appl. Mater. Interfaces*, 2023, **15**(19), 23058–23067.
- H. Li, Q. Wan, C. Du, J. Zhao, F. Li, Y. Zhang, Y. Zheng, M. Chen, K. H. L. Zhang, J. Huang, G. Fu, S. Lin, X. Huang and H. Xiong, *Nat. Commun.*, 2022, **13**, 6072.
- D. E. Doronkin, S. Wang, D. I. Sharapa, B. J. Deschner, T. L. Sheppard, A. Zimina, F. Studt, R. Dittmeyer, S. Behrens and J. Grunwaldt, *Catal. Sci. Technol.*, 2020, **10**, 4726–4742.
- W. Tian, Y. Dong, H. Qin, Z. Luo, Q. Lin, Z. Chen, H. Pan, Y. Shi and K. Wang, *Mol. Catal.*, 2023, **547**, 113376.
- R. J. Lewis, K. Ueura, Y. Fukuta, S. J. Freakley, L. Kang, R. Wang, Q. He, J. K. Edwards, D. J. Morgan, Y. Yamamoto and G. J. Hutchings, *ChemCatChem*, 2019, **11**, 1673–1680.
- X. Hu, Q. Xie, J. Zhang, Q. Yu, H. Liu and Y. Sun, *Int. J. Hydrogen Energy*, 2020, **45**, 27837–27845.
- A. Santos, R. J. Lewis, G. Malta, A. G. R. Howe, D. J. Morgan, E. Hampton, P. Gaskin and G. J. Hutchings, *Ind. Eng. Chem. Res.*, 2019, **58**, 12623–12631.
- J. K. Edwards, A. Thomas, A. F. Carley, A. A. Herzing, C. J. Kiely and G. J. Hutchings, *Green Chem.*, 2008, **10**, 388–394.
- S. Kanungo, L. van Haandel, E. J. M. Hensen, J. C. Schouten and M. Fernanda Neira d'Angelo, *J. Catal.*, 2019, **370**, 200–209.
- J. Edwards, B. Solsona, P. Landon, A. Carley, A. Herzing, C. Kiely and G. Hutchings, *J. Catal.*, 2005, **236**, 69–79.
- R. Burch and P. R. Ellis, *Appl. Catal., B*, 2003, **42**, 203–211.
- V. R. Choudhary, A. G. Gaikwad and S. D. Sansare, *Catal. Lett.*, 2002, **83**, 235–239.



- 43 X. Gong, R. J. Lewis, S. Zhou, D. J. Morgan, T. E. Davies, X. Liu, C. J. Kiely, B. Zong and G. J. Hutchings, *Catal. Sci. Technol.*, 2020, **10**, 4635–4644.
- 44 F. Wang, C. Xia, S. P. de Visser and Y. Wang, *J. Am. Chem. Soc.*, 2019, **141**, 901–910.
- 45 J. Brehm, R. J. Lewis, T. Richards, T. Qin, D. J. Morgan, T. E. Davies, L. Chen, X. Liu and G. J. Hutchings, *ACS Catal.*, 2022, **12**(19), 11777–11789.
- 46 S. Yu, X. Cheng, Y. Wang, B. Xiao, Y. Xing, J. Ren, Y. Lu, H. Li, C. Zhuang and G. Chen, *Nat. Commun.*, 2022, **13**, 4737.
- 47 P. Tian, D. Ding, Y. Sun, F. Xuan, X. Xu, J. Xu and Y. Han, *J. Catal.*, 2019, **369**, 95–104.
- 48 C. Williams, J. H. Carter, N. F. Dummer, Y. K. Chow, D. J. Morgan, S. Yacob, P. Serna, D. J. Willock, R. J. Meyer, S. H. Taylor and G. J. Hutchings, *ACS Catal.*, 2018, **8**, 2567–2576.

